I&EC research
Industrial & Engineering Chemistry Research

Article

pubs.acs.org/IECR

Near-Infrared Responsive MoS_2/Poly(*N*-isopropylacrylamide) Hydrogels for Remote Light-Controlled Microvalves

Junyang Zhang, Ping Du, Danyun Xu, Yang Li, Wenchao Peng, Guoliang Zhang, Fengbao Zhang,* and Xiaobin Fan*

School of Chemical Engineering and Technology, State Key Laboratory of Chemical Engineering, Collaborative Innovation Center of Chemical Science and Engineering, Tianjin University, Tianjin 300072, China

Supporting Information

ABSTRACT: To achieve remote control over the swelling/deswelling transition, chemically exfoliated MoS_2 nanosheets with photothermal properties are successfully incorporated into poly(*N*-isopropylacrylamide) (PNIPAM) hydrogel by in situ polymerization. Different from the conventional thermal-responsive PNIPAM hydrogel, the MoS_2/PNIPAM composite hydrogel here shows a reversible volumetric change in response to near-infrared (NIR) illumination. Based on this new composite hydrogel, a microfluidic device actuated remotely by NIR laser is also demonstrated.

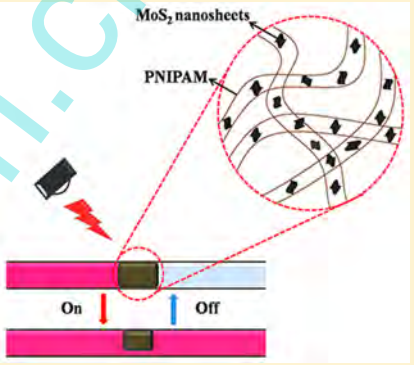

INTRODUCTION

Responsive hydrogels which show phase transitions under external stimulus (e.g., temperature, pH, and photons) have attracted increasing attention due to their potential applications in drug delivery, microlenses, microdevices, etc.[1−7] In particular, poly(*N*-isopropylacrylamide) (PNIPAM) hydrogel has emerged as one of the most popular thermal-responsive hydrogels since it undergoes a dramatic swelling transition at its lower critical solution temperature (LCST).[8,9] However, the application of PNIPAM hydrogel is still limited by its simple thermal responsiveness, which is not desirable for remote control, especially for the applications in microdevices. Incorporating photothermal conversion materials into the PNIPAM hydrogels can endow the composite hydrogel with near-infrared (NIR)-responsive properties and achieve remote control by light, a stimulus with tunable intensity and wavelength.[10−13] In particular, actuation has been demonstrated by a combination of the near-infrared (NIR) absorption of nanomaterials and the reversible swelling/deswelling transition in the PNIPAM hydrogel.[14−18]

Given the exceptional surface-area-to mass ratio, two-dimensional (2D) materials are promising NIR photothermal candidates that can be loaded with high cargo concentrations.[19] For example, graphene and its derivatives have showed impressive photothermal properties and potential applications in many fields.[20,21] However, the hydrophobic nature of graphene (or reduced graphene oxide) makes them difficult to incorporate with PNIPAM, and the efficacy of the hydrophilic graphene oxide is still under debate.[22−28] For example, in Robinson's opinion,[29] the high dose/power needed for photoablation was due to the suboptimal absorption of NIR light by graphene oxide (GO) in a highly oxidized form. The photothermal conversion efficiency of GO is relatively low due to the existence of abundant structural defects. Therefore, searching for new 2D candidates with excellent photothermal properties and good compatibility with PNIPAM is still an urgent task.

As a 2D analogue of graphene, exfoliated MoS_2 has showed promising applications in photothermal therapy.[30−32] Considering the hydrophilic nature of the chemically exfoliated MoS_2, we thought that it might be used as an ideal candidate to incorporate into the PNIPAM hydrogel. To test this idea, we successfully prepared the MoS_2/PNIPAM composite hydrogel by a simple in situ polymerization method, and a microfluidic device actuated remotely by NIR laser was also demonstrated (Scheme 1).

EXPERIMENTAL SECTION

Synthesis of Chemically Exfoliated MoS_2. Chemical exfoliation of MoS_2 was adapted from our recent method.[33] In a typical procedure, 1 g of MoS_2 powder was immersed in 10 mL of *n*-butyllithium (2.5 M in hexane) and sonicated (120 W) in a 50 mL Schlenk flask for 3 h. The intercalated samples were retrieved by centrifugation and washed three times using hexane to remove excess lithium and organic residues. The centrifugation process should be accomplished within 1/2 h.

Received: January 30, 2016
Revised: March 26, 2016
Accepted: April 8, 2016
Published: April 8, 2016

DOI: 10.1021/acs.iecr.6b00432
Ind. Eng. Chem. Res. 2016, 55, 4526−4531

Scheme 1. Illustration for the MoS_2/PNIPAM Hydrogel-Based Light-Controlled Microvalve

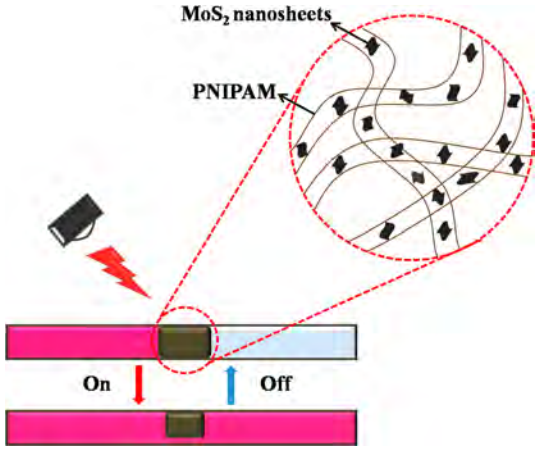

Standard air-free techniques were employed by using a Schlenk line or a glovebox under the protection of inert gas. Then the intercalated samples were dried with argon blowing, followed by exfoliation and sonication in distilled water for about 30 min. The exfoliated samples were purified by centrifugation with water and collected for further use.

Synthesis of MoS_2/PNIPAM Nanocomposite Hydrogels. First, 700 mg of *N*-isopropylacrylamide monomer and 6 mg of *N*,*N*′-methylenebis(acrylamide) cross-linker were dissolved in 10 mL of 0.5 mg mL^{-1} or 1 mg mL^{-1} homogeneous MoS_2 aqueous dispersion in an ice bath with stirring. The mixture was bubbled with Ar gas for 30 min to remove any residual oxygen. Then, 10 μL of *N*,*N*,*N*′,*N*′-tetramethylethylenediamine as a polymerization accelerator and 20 μL of ammonium peroxodisulfate aqueous initiator solution (20 wt %) were added successively. The polymerization was completed in a centrifugal tube for 24 h at room temperature. The obtained hydrogels were washed by deionized water to remove the excess monomer and MoS_2. The pure PNIPAM hydrogels were also synthesized in distilled water in the absence of MoS_2. The overall loading ($\leq$1 mg mL^{-1}) is restricted by the intrinsic dispersibility of MoS_2 and interaction of raw materials.

Fabrication of Microvalves. To fabricate the hydrogel microvalves in the microfluidic channels, a cylindrical fragment of MoS_2/PNIPAM hydrogel was inserted into a quartz tube of 2.5 mm inner diameter. Red rhodamine B solution and distilled water were respectively introduced to the two sides of the quartz tube and separated by the hydrogel. When exposed to the 808 nm laser (0.8 W) for 2 min, the composite hydrogel shrank to allow for the fluidic flow, and the color of the water changed.

Characterization. Samples were characterized by atomic force microscopy (AFM; CSPM 5000), UV−vis−NIR spectroscopy (Unico, UV-3802), scanning electron microscopy (SEM; FEI NOVA NanoSEM430), energy dispersive X-ray spectroscopy (EDX; FEI NOVA NanoSEM 430), Raman spectroscopy (Renishaw inVia reflex Raman spectrometer with 532 nm laser excitation), and X-ray photoelectron spectroscopy (XPS; PerkinElmer, PHI 1600spectrometer).

To determine the swelling ratio (S_r) of hydrogels, all samples were immersed in water and equilibrated for 2 days at various temperatures. S_r was calculated via the following equation:

$$S_r = (W_w - W_d)/W_d$$

where W_w and W_d are the hydrogel masses in the wet state and dry state, respectively. Differential scanning calorimetry (DSC; DSC 1/500, Mettler-Toledo, Switzerland) was carried out under a N_2 atmosphere at a heating rate of 1.0 °C/min.

RESULTS AND DISCUSSION

The aqueous dispersion of chemically exfoliated MoS_2 nanosheets was obtained by our sonication-assisted intercalation method.[33] Atomic force microscopy (AFM) confirms that abundant exfoliated MoS_2 nanosheets with lateral sizes of micrometers are suspended in the dispersion (Figure 1a).

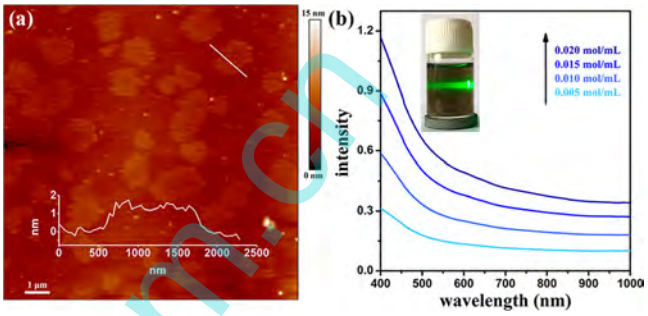

Figure 1. Typical AFM images of chemically exfoliated MoS_2 nanosheets (a) and their UV−vis−NIR absorbance spectra with different concentrations in water (b). Inset: digital photograph of chemically exfoliated MoS_2 dispersion in water.

Cross-section analysis reveals these nanosheets have the same apparent AFM height of ~1.3 nm, indicating their monolayer nature. Note that the apparent height here is somewhat larger than the theoretical thickness of monolayer MoS_2, attributed to the intrinsic out-of-plane deformation of 2D materials and the possible presence of trapped solvent (H_2O).[34,35] Different from the MoS_2 nanosheets directly exfoliated from the bulk MoS_2 crystals by ultrasonication or shear mixing,[36−39] the chemically exfoliated MoS_2 nanosheets have mainly the 1T phase, which shows strong and featureless absorbance in the vis−NIR region (Figure 1b). Actually, the mass extinction coefficient of the chemically exfoliated MoS_2 nanosheets at 800 nm can be calculated to be 22.4 L g^{-1} cm^{-1}. This value is comparable to that of graphene (24.6 L g^{-1} cm^{-1}) and much larger than that of GO (3.6 L g^{-1} cm^{-1}),[40] indicating the high efficacy of the chemically exfoliated MoS_2 nanosheets as NIR photothermal agents.

To prepare the MoS_2/PNIPAM composite hydrogels, cross-linking of the *N*-isopropylacrylamide monomer (NIPAM) was carried out in the homogeneous MoS_2 aqueous dispersion at room temperature. Although the final concentration of MoS_2 in the composite hydrogels could reach over 1 mg mL^{-1}, latter systematic studies showed that the ideal loading of MoS_2 should be around 0.5 mg mL^{-1}. As shown in Figure 2a (inset), the composite hydrogel shows a dramatic color change (homogeneous black) when compared with the pure PNIPAM hydrogel (transparent), indicating the good dispersion of MoS_2 in the hydrogel matrix. This speculation was supported by scanning electron microscopy (SEM) and corresponding elemental mapping. Similar to the pure PNIPAM hydrogel (Figure S1, Supporting Information), the freeze-dried composite hydrogel (with 0.5 mg mL^{-1} MoS_2) exhibits a macroporous structure with highly interconnected pores (Figure 2a), indicating the MoS_2 nanosheets do not impact the microstructure of hydrogel. Corresponding energy dispersive X-ray

DOI: 10.1021/acs.iecr.6b00432
Ind. Eng. Chem. Res. 2016, 55, 4526−4531

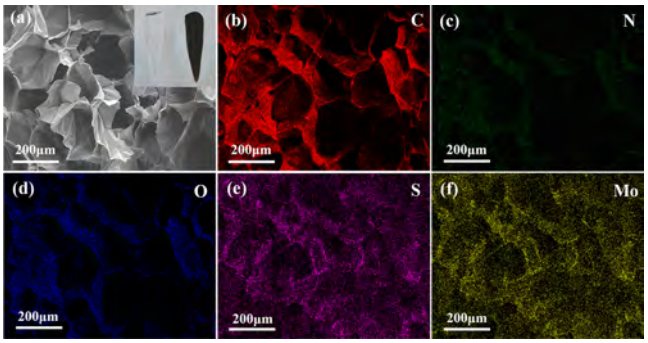

Figure 2. SEM images of freeze-dried MoS_2/PNIPAM composite hydrogel (a) and corresponding quantitative EDS element mapping of C (b), N (c), O (d), S (e), and Mo (f). Inset: digital photographs of a pure PNIPAM (left) and the MoS_2/PNIPAM composite hydrogel with 0.5 mg/mL MoS_2 (right).

spectroscopy (EDS) mapping confirmed that elemental C, N, O, S, and Mo were homogeneously distributed in the whole matrix (Figure 2b–f), demonstrating the homogeneous distribution of MoS_2.

Interestingly, the composite hydrogel shows negligible S and Mo signals in the X-ray photoelectron spectroscopy (XPS) spectrum (Figure S3, Supporting Information). Considering the limited penetration depth (several nanometers) of XPS, this result suggests the successful wrapping of the MoS_2 nanosheets inside the PNIPAM network. Actually, the Raman peaks of the exfoliated MoS_2 can be easily observed in the MoS_2/PNIPAM composite hydrogel (Figure 3a). Similar to the exfoliated MoS_2 precursors (black line), the composite hydrogel sample (blue line) displays the typical in-plane E^1_{2g} mode and out-of-plane A_{1g} mode of MoS_2,[41] despite their slight blue shift (~2 cm^{-1}) caused by the local strain. The additional J_1, J_2, and J_3 peaks were attributed to the distorted superlattice structure of 1T MoS_2, in line with previous studies.[42]

To evaluate the responsiveness of the composite hydrogels, we measured their swelling ratios under different temperatures, with the pure PNIPAM hydrogel as a control. As shown in Figure 3b, repeated experiments demonstrated that all of the samples had similar temperature sensitivity and high swelling ratios below the LCST. Actually, the introduction of a limited amount of MoS_2 nanosheets (0.5 mg mL^{-1}) can slightly increase the swelling ratio of the hydrogel, while further increase of the MoS_2 concentration (e.g., 1 mg mL^{-1}) will result in the decrease of the swelling and deswelling capacity. This phenomenon may be explained by the increased interaction between PNIPAM and excessive MoS_2 nanosheets, which may hamper the coil-to-globule transition of the PNIPAM. The corresponding LCST of the hydrogels was determined by using differential scanning calorimetry (DSC). We found that all the endothermic peaks of the hydrogels appeared around 34.1 °C (Figure 3c), corresponding to the same LCST.[15] This result means the embedding of MoS_2

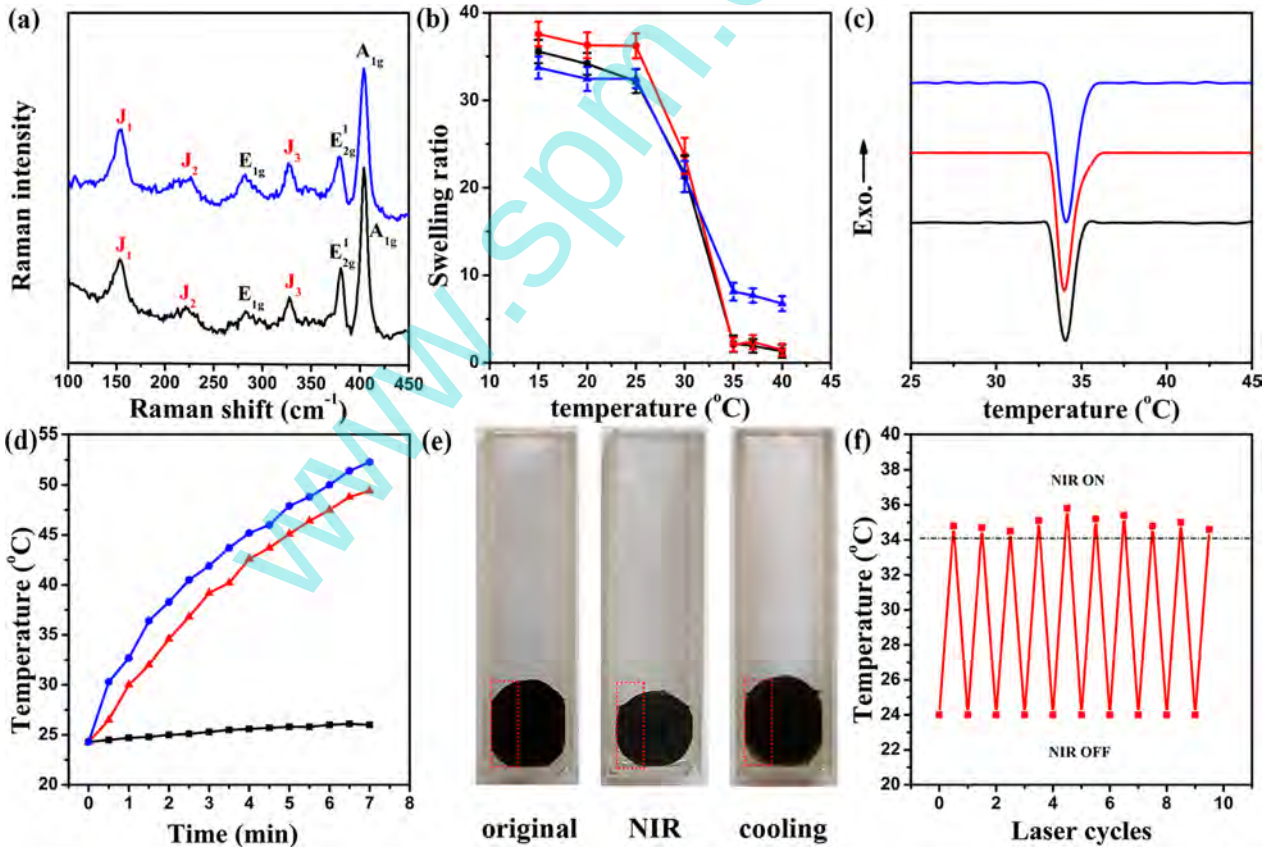

Figure 3. (a) Raman spectra for MoS_2 (black) and MoS_2/PNIPAM with 0.5 mg mL^{-1} MoS_2 (blue). (b) Swelling ratio dependence on temperature for pure PNIPAM (black) and MoS_2/PNIPAM with 0.5 (red) and 1 mg mL^{-1} (blue) MoS_2. (c) DSC thermograms of pure PNIPAM (black) and MoS_2/PNIPAM with 0.5 (red) and 1 mg mL^{-1} (blue) MoS_2. (d) Temperature of surrounding water (0.5 mL) with pure PNIPAM (black) and MoS_2/PNIPAM prepared with 0.5 (red) and 1 mg mL^{-1} (blue). (e) Photograph of volume change of MoS_2/PNIPAM with and without NIR irradiation. (f) Temperature changes of MoS_2/PNIPAM with 0.5 mg mL^{-1} MoS_2 as a function of heating–cooling cycle.

DOI: 10.1021/acs.iecr.6b00432
Ind. Eng. Chem. Res. 2016, 55, 4526–4531

nanosheets has virtually no effect on the phase transition temperature of the PNIPAM network. Different from the other photothermal nanomaterials,[16,43] MoS_2 has no oxygen-containing functional group to form hydrogen bonds with H_2O or PNIPAM chains. Besides, the hydrophilic nature of the chemical exfoliated MoS_2 cannot introduce additional hydrophobic forces to PNIPAM. Therefore, there is no obvious change of LCST and swelling ratio. Similarly, the hysteresis of the hydrogels is not affected by MoS_2 (Figure S5, Supporting Information). Note that the swelling of the composite hydrogel as a function of repeated cycles demonstrates that it has good reusability. Besides, the number of layers of MoS_2 is not changed even after five swell−deswell cycles (Figures S6 and S7, Supporting Information).

In order to investigate the photothermal properties, 0.5 mL of water with 0.4 cm^3 of the as-prepared hydrogels was exposed to an 808 nm NIR laser at a power of 0.8 W. For the surrounding water with MoS_2/PNIPAM hydrogels, the fast temperature rise tendency on increasing MoS_2 loading and irradiation time (0−7 min) is shown in Figure 3d. In contrast, water with pure PNIPAM hydrogel (black line) exhibits no obvious temperature change under the same conditions, confirming that the MoS_2 is the main light-absorbing agent. In line with previous studies with other photothermal agents,[22,44] we found that the concentration of MoS_2 in the composite hydrogels could be used to control the increase of the NIR-induced temperature. However, considering the negative effects of excessive MoS_2 on the swelling and deswelling capacity of the composite hydrogels as discussed above, a MoS_2 loading of 0.5 mg mL^{-1} should be preferred for the volume transition in the light-controlled microvalve.

As illustrated in Figure 3e, the MoS_2/PNIPAM composite hydrogel shows significant volume reduction under NIR irradiation, attributed to the transition from a hydrophilic swollen state to a hydrophobic collapsed state of the PNIPAM.[45,46] When the laser was turned off, however, the nanocomposite hydrogel could return to its initial size by reabsorbing water. The stability and reusability of the composite hydrogels were also tested. During repeated laser exposure and nonexposure cycles, the temperature changes of the composite hydrogel were completely reversible (Figure 3f). Moreover, the surrounding water could reach the LCST (34.1 °C) in 2 min, and the temperature inside the composite hydrogel should be higher. It should be noted that the phase of the MoS_2 nanosheets in the composite hydrogel remains unchanged, even after prolonged irradiation for 1 h (Figure S3, Supporting Information). These results suggest that the MoS_2/PNIPAM composite hydrogels can be remotely controlled by NIR and have promising applications in many fields.

For example, based on the excellent photothermal properties of the composite hydrogels, a liquid microvalve was fabricated to control the flow in a microfluidic channel by NIR irradiation. For illustration purposes, rhodamine B solution (red) and distilled water were separated by the hydrogels inside the quartz tubes. As shown in Figure 4a, for its "OFF" state, the composite hydrogel microvalve completely blocked the flow in the microfluidic channel. The effectiveness of the microvalves has been also tested, and we confirm that the hydrogel could block the fluid for at least 15 days (Figure S8, Supporting Information). When the NIR laser was turned on (the "ON" state), the composite hydrogel contracted to allow fluid flow, resulting in the color change shown in Figure 4b. Despite the difficulty of comparison, the microvalve here can be efficiently controlled by NIR irradiation with much lower intensity, when compared with previous study on the GO/PNIPAM system.[22] Note that the hydrogel microvalve could return to ambient temperature and recovered its initial size as the NIR light was turned off, and thereby blocked the fluid flow again. As a contrast, the pure PNIPAM hydrogel continued to block the flow even after irradiation (Figure 4c,d).

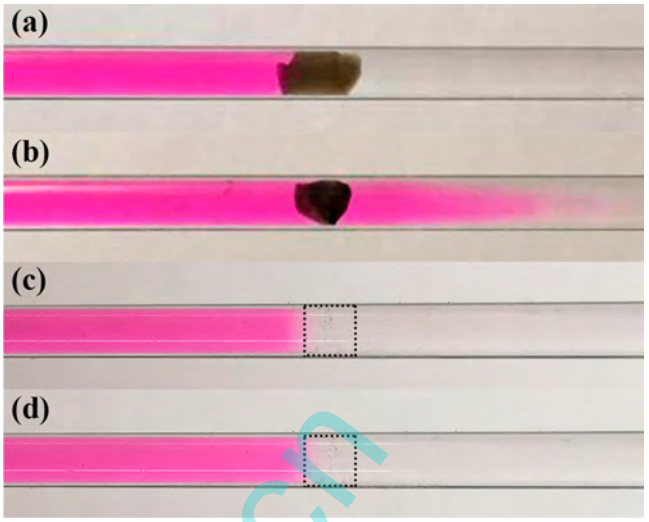

Figure 4. Liquid microvalve fabricated by the MoS_2/PNIPAM composite hydrogel (a, b) and pure PNIPAM hydrogel (c, d). The photographs show the microvalve before (a, c) and after (b, d) exposure to NIR irradiation (808 nm, 0.8 W) for 2 min. The solutions encapsulated in the left and right sides are a red rhodamine solution and water, respectively.

CONCLUSIONS

In summary, we developed a facile in situ method for embedding chemically exfoliated MoS_2 nanosheets into the PNIPAM network. The obtained MoS_2/PNIPAM composite hydrogel exhibits NIR-responsive properties with a superior photothermal efficacy. Its swelling/deswelling process not only can be remotely controlled by NIR irradiation, but also is completely reversible. To explore its applications, we fabricated a liquid microvalve with this new composite hydrogel and illustrated the successful activation by NIR laser. This novel light-activated PNIPAM−MoS_2 system may also find promising applications in drug delivery, sensors, smart catalytics, etc.

ASSOCIATED CONTENT

Supporting Information

The Supporting Information is available free of charge on the ACS Publications website at DOI: 10.1021/acs.iecr.6b00432.

SEM images, XPS spectra, Raman spectra of the composite hydrogels (PDF)

AUTHOR INFORMATION

Corresponding Authors

*E-mail: fbzhang@tju.edu.cn (F.Z.).
*E-mail: xiaobinfan@tju.edu.cn (X.F.).

Notes

The authors declare no competing financial interest.

DOI: 10.1021/acs.iecr.6b00432
Ind. Eng. Chem. Res. 2016, 55, 4526−4531

■ ACKNOWLEDGMENTS

This study is supported by the National Natural Science Funds for Excellent Young Scholars (No. 21222608), the Foundation for the Author of National Excellent Doctoral Dissertation of China (No. 201251), the Program for New Century Excellent Talents in University (No. NCET-12-0392), and the Program of Introducing Talents of Discipline to Universities (No. B06006).

■ REFERENCES

(1) Jochum, F. D.; Theato, P. Temperature- and light-responsive smart polymer materials. *Chem. Soc. Rev.* **2013**, *42*, 7468−7483.
(2) Koetting, M. C.; Peters, J. T.; Steichen, S. D.; Peppas, N. A. Stimulus-responsive hydrogels: Theory, modern advances, and applications. *Mater. Sci. Eng., R* **2015**, *93*, 1−49.
(3) Chan, K. W. Y.; Liu, G. S.; Song, X. L.; Kim, H.; Yu, T.; Arifin, D. R.; Gilad, A. A.; Hanes, J.; Walczak, P.; van Zijl, P. C. M.; Bulte, J. W. M.; McMahon, M. T. MRI-detectable pH nanosensors incorporated into hydrogels for in vivo sensing of transplanted-cell viability. *Nat. Mater.* **2013**, *12*, 268−275.
(4) Alvarez-Lorenzo, C.; Concheiro, A. Smart drug delivery systems: from fundamentals to the clinic. *Chem. Commun.* **2014**, *50*, 7743−7765.
(5) Dong, L.; Agarwal, A. K.; Beebe, D. J.; Jiang, H. R. Adaptive liquid microlenses activated by stimuli-responsive hydrogels. *Nature* **2006**, *442*, 551−554.
(6) Qiu, Y.; Park, K. Environment-sensitive hydrogels for drug delivery. *Adv. Drug Delivery Rev.* **2012**, *64*, 49−60.
(7) Satarkar, N. S.; Zhang, W. L.; Eitel, R. E.; Hilt, J. Z. Magnetic hydrogel nanocomposites as remote controlled microfluidic valves. *Lab Chip* **2009**, *9*, 1773−1779.
(8) Ramos, J.; Imaz, A.; Forcada, J. Temperature-sensitive nanogels: poly(N-vinylcaprolactam) versus poly(N-isopropylacrylamide). *Polym. Chem.* **2012**, *3*, 852−856.
(9) Wang, W.; Tian, X.; Feng, Y.; Cao, B.; Yang, W.; Zhang, L. Thermally On-Off Switching Membranes Prepared by Pore-Filling Poly(N-isopropylacrylamide) Hydrogels. *Ind. Eng. Chem. Res.* **2010**, *49*, 1684−1690.
(10) Hauser, A. W.; Evans, A. A.; Na, J. H.; Hayward, R. C. Photothermally Reprogrammable Buckling of Nanocomposite Gel Sheets. *Angew. Chem., Int. Ed.* **2015**, *54*, 5434−5437.
(11) Lee, E.; Lee, H.; Yoo, S. I.; Yoon, J. Photothermally Triggered Fast Responding Hydrogels Incorporating a Hydrophobic Moiety for Light-Controlled Microvalves. *ACS Appl. Mater. Interfaces* **2014**, *6*, 16949−16955.
(12) Sugiura, S.; Szilagyi, A.; Sumaru, K.; Hattori, K.; Takagi, T.; Filipcsei, G.; Zrinyi, M.; Kanamori, T. On-demand microfluidic control by micropatterned light irradiation of a photoresponsive hydrogel sheet. *Lab Chip* **2009**, *9*, 196−198.
(13) ter Schiphorst, J.; Coleman, S.; Stumpel, J. E.; Ben Azouz, A.; Diamond, D.; Schenning, A. Molecular Design of Light-Responsive Hydrogels, For in Situ Generation of Fast and Reversible Valves for Microfluidic Applications. *Chem. Mater.* **2015**, *27*, 5925−5931.
(14) Sershen, S. R.; Mensing, G. A.; Ng, M.; Halas, N. J.; Beebe, D. J.; West, J. L. Independent optical control of microfluidic valves formed from optomechanically responsive nanocomposite hydrogels. *Adv. Mater.* **2005**, *17*, 1366−1368.
(15) Fujigaya, T.; Morimoto, T.; Niidome, Y.; Nakashima, N. NIR Laser-Driven Reversible Volume Phase Transition of Single-Walled Carbon Nanotube/Poly(N-isopropylacrylamide) Composite Gels. *Adv. Mater.* **2008**, *20*, 3610−3614.
(16) Li, W.; Wang, J. S.; Ren, J. S.; Qu, X. G. 3D Graphene Oxide-Polymer Hydrogel: Near-Infrared Light-Triggered Active Scaffold for Reversible Cell Capture and On-Demand Release. *Adv. Mater.* **2013**, *25*, 6737−6743.
(17) Shi, K.; Liu, Z.; Wei, Y.-Y.; Wang, W.; Ju, X.-J.; Xie, R.; Chu, L.-Y. Near-Infrared Light-Responsive Poly(N-isopropylacrylamide)/Graphene Oxide Nanocomposite Hydrogels with Ultrahigh Tensibility. *ACS Appl. Mater. Interfaces* **2015**, *7*, 27289−27298.
(18) Jadhav, A. D.; Yan, B.; Luo, R. C.; Wei, L.; Zhen, X.; Chen, C. H.; Shi, P. Photoresponsive microvalve for remote actuation and flow control in microfluidic devices. *Biomicrofluidics* **2015**, *9*, 034114.
(19) Chen, Y.; Tan, C. L.; Zhang, H.; Wang, L. Z. Two-dimensional graphene analogues for biomedical applications. *Chem. Soc. Rev.* **2015**, *44*, 2681−2701.
(20) Yang, K.; Feng, L. Z.; Shi, X. Z.; Liu, Z. Nano-graphene in biomedicine: theranostic applications. *Chem. Soc. Rev.* **2013**, *42*, 530−547.
(21) Pan, Y. Z.; Bao, H. Q.; Sahoo, N. G.; Wu, T. F.; Li, L. Water-Soluble Poly(N-isopropylacrylamide)-Graphene Sheets Synthesized via Click Chemistry for Drug Delivery. *Adv. Funct. Mater.* **2011**, *21*, 2754−2763.
(22) Zhu, C. H.; Lu, Y.; Peng, J.; Chen, J. F.; Yu, S. H. Photothermally Sensitive Poly(N-isopropylacrylamide)/Graphene Oxide Nanocomposite Hydrogels as Remote Light-Controlled Liquid Microvalves. *Adv. Funct. Mater.* **2012**, *22*, 4017−4022.
(23) Zhang, E. Z.; Wang, T.; Hong, W.; Sun, W. X.; Liu, X. X.; Tong, Z. Infrared-driving actuation based on bilayer graphene oxide-poly(N-isopropylacrylamide) nanocomposite hydrogels. *J. Mater. Chem. A* **2014**, *2*, 15633−15639.
(24) Zhang, J.; Song, L.; Zhang, Z. P.; Chen, N.; Qu, L. T. Environmentally Responsive Graphene Systems. *Small* **2014**, *10*, 2151−2164.
(25) Hou, C. Y.; Zhang, Q. H.; Wang, H. Z.; Li, Y. G. Functionalization of PNIPAAm microgels using magnetic graphene and their application in microreactors as switch materials. *J. Mater. Chem.* **2011**, *21*, 10512−10517.
(26) Sun, S. T.; Wu, P. Y. A one-step strategy for thermal- and pH-responsive graphene oxide interpenetrating polymer hydrogel networks. *J. Mater. Chem.* **2011**, *21*, 4095−4097.
(27) Hao, N.; Li, J. Y.; Xiong, M.; Xia, X. H.; Xu, J. J.; Chen, H. Y. Remote Control of Reversible Localized Protein Adsorption in Microfluidic Devices. *ACS Appl. Mater. Interfaces* **2014**, *6*, 11869−11873.
(28) Konkena, B.; Vasudevan, S. Understanding Aqueous Dispersibility of Graphene Oxide and Reduced Graphene Oxide through pK(a) Measurements. *J. Phys. Chem. Lett.* **2012**, *3*, 867−872.
(29) Robinson, J. T.; Tabakman, S. M.; Liang, Y.; Wang, H.; Sanchez Casalongue, H.; Vinh, D.; Dai, H. Ultrasmall Reduced Graphene Oxide with High Near-Infrared Absorbance for Photothermal Therapy. *J. Am. Chem. Soc.* **2011**, *133*, 6825−6831.
(30) Liu, T.; Wang, C.; Gu, X.; Gong, H.; Cheng, L.; Shi, X. Z.; Feng, L. Z.; Sun, B. Q.; Liu, Z. Drug Delivery with PEGylated MoS_2 Nanosheets for Combined Photothermal and Chemotherapy of Cancer. *Adv. Mater.* **2014**, *26*, 3433−3440.
(31) Liu, T.; Wang, C.; Cui, W.; Gong, H.; Liang, C.; Shi, X. Z.; Li, Z. W.; Sun, B. Q.; Liu, Z. Combined photothermal and photodynamic therapy delivered by PEGylated MoS_2 nanosheets. *Nanoscale* **2014**, *6*, 11219−11225.
(32) Liu, T.; Shi, S. X.; Liang, C.; Shen, S. D.; Cheng, L.; Wang, C.; Song, X. J.; Goel, S.; Barnhart, T. E.; Cai, W. B.; Liu, Z. Iron Oxide Decorated MoS_2 Nanosheets with Double PEGylation for Chelator-Free Radio labeling and Multimodal Imaging Guided Photothermal Therapy. *ACS Nano* **2015**, *9*, 950−960.
(33) Fan, X.; Xu, P.; Zhou, D.; Sun, Y.; Li, Y. C.; Nguyen, M. A. T.; Terrones, M.; Mallouk, T. E. Fast and Efficient Preparation of Exfoliated 2H MoS_2 Nanosheets by Sonication-Assisted Lithium Intercalation and Infrared Laser-Induced 1T to 2H Phase Reversion. *Nano Lett.* **2015**, *15*, 5956−5960.
(34) Brivio, J.; Alexander, D. T. L.; Kis, A. Ripples and Layers in Ultrathin MoS_2 Membranes. *Nano Lett.* **2011**, *11*, 5148−5153.
(35) Backes, C.; Smith, R. J.; McEvoy, N.; Berner, N. C.; McCloskey, D.; Nerl, H. C.; O'Neill, A.; King, P. J.; Higgins, T.; Hanlon, D.; Scheuschner, N.; Maultzsch, J.; Houben, L.; Duesberg, G. S.; Donegan, J. F.; Nicolosi, V.; Coleman, J. N. Edge and confinement effects allow

DOI: 10.1021/acs.iecr.6b00432
Ind. Eng. Chem. Res. 2016, 55, 4526−4531

in situ measurement of size and thickness of liquid-exfoliated nanosheets. *Nat. Commun.* **2014**, *5*, 4576.
(36) Coleman, J. N.; Lotya, M.; O'Neill, A.; Bergin, S. D.; King, P. J.; Khan, U.; Young, K.; Gaucher, A.; De, S.; Smith, R. J.; Shvets, I. V.; Arora, S. K.; Stanton, G.; Kim, H. Y.; Lee, K.; Kim, G. T.; Duesberg, G. S.; Hallam, T.; Boland, J. J.; Wang, J. J.; Donegan, J. F.; Grunlan, J. C.; Moriarty, G.; Shmeliov, A.; Nicholls, R. J.; Perkins, J. M.; Grieveson, E. M.; Theuwissen, K.; McComb, D. W.; Nellist, P. D.; Nicolosi, V. Two-Dimensional Nanosheets Produced by Liquid Exfoliation of Layered Materials. *Science* **2011**, *331*, 568−571.
(37) Paton, K. R.; Varrla, E.; Backes, C.; Smith, R. J.; Khan, U.; O'Neill, A.; Boland, C.; Lotya, M.; Istrate, O. M.; King, P.; Higgins, T.; Barwich, S.; May, P.; Puczkarski, P.; Ahmed, I.; Moebius, M.; Pettersson, H.; Long, E.; Coelho, J.; O'Brien, S. E.; McGuire, E. K.; Sanchez, B. M.; Duesberg, G. S.; McEvoy, N.; Pennycook, T. J.; Downing, C.; Crossley, A.; Nicolosi, V.; Coleman, J. N. Scalable production of large quantities of defect-free few-layer graphene by shear exfoliation in liquids. *Nat. Mater.* **2014**, *13*, 624−630.
(38) Li, H.; Wu, J. M. T.; Yin, Z. Y.; Zhang, H. Preparation and Applications of Mechanically Exfoliated Single-Layer and Multi layer MoS_2 and WSe_2 Nanosheets. *Acc. Chem. Res.* **2014**, *47*, 1067−1075.
(39) Yao, Y. G.; Tolentino, L.; Yang, Z. Z.; Song, X. J.; Zhang, W.; Chen, Y. S.; Wong, C. P. High-Concentration Aqueous Dispersions of MoS_2. *Adv. Funct. Mater.* **2013**, *23*, 3577−3583.
(40) Chou, S. S.; Kaehr, B.; Kim, J.; Foley, B. M.; De, M.; Hopkins, P. E.; Huang, J.; Brinker, C. J.; Dravid, V. P. Chemically Exfoliated MoS_2 as Near-Infrared Photothermal Agents. *Angew. Chem., Int. Ed.* **2013**, *52*, 4160−4164.
(41) Zhang, X.; Qiao, X. F.; Shi, W.; Wu, J. B.; Jiang, D. S.; Tan, P. H. Phonon and Raman scattering of two-dimensional transition metal dichalcogenides from monolayer, multilayer to bulk material. *Chem. Soc. Rev.* **2015**, *44*, 2757−2785.
(42) Jiménez Sandoval, S.; Yang, D.; Frindt, R. F.; Irwin, J. C. Raman study and lattice dynamics of single molecular layers of MoS_2. *Phys. Rev. B: Condens. Matter Mater. Phys.* **1991**, *44*, 3955−3962.
(43) Satarkar, N. S.; Johnson, D.; Marrs, B.; Andrews, R.; Poh, C.; Gharaibeh, B.; Saito, K.; Anderson, K. W.; Hilt, J. Z. Hydrogel-MWCNT Nanocomposites: Synthesis, Characterization, and Heating with Radiofrequency Fields. *J. Appl. Polym. Sci.* **2010**, *117*, 1813−1819.
(44) Charati, M. B.; Lee, I.; Hribar, K. C.; Burdick, J. A. Light-Sensitive Polypeptide Hydrogel and Nanorod Composites. *Small* **2010**, *6*, 1608−1611.
(45) Yao, C.; Liu, Z.; Yang, C.; Wang, W.; Ju, X. J.; Xie, R.; Chu, L. Y. Poly(N-isopropylacrylamide)-Clay Nanocomposite Hydrogels with Responsive Bending Property as Temperature-Controlled Manipulators. *Adv. Funct. Mater.* **2015**, *25*, 2980−2991.
(46) Wang, M.; Gao, Y.; Cao, C.; Chen, K.; Wen, Y.; Fang, D.; Li, L.; Guo, X. Binary Solvent Colloids of Thermosensitive Poly(N-isopropylacrylamide) Microgel for Smart Windows. *Ind. Eng. Chem. Res.* **2014**, *53*, 18462−18472.

DOI: 10.1021/acs.iecr.6b00432
Ind. Eng. Chem. Res. 2016, 55, 4526−4531